2009 American Control Conference
Hyatt Regency Riverfront, St. Louis, MO, USA
June 10-12, 2009

Mixing Enhancement in 2D Magnetohydrodynamic Channel Flow by Extremum Seeking Boundary Control

Lixiang Luo and Eugenio Schuster

Abstract— **The interaction between electrically conducting fluids and magnetic fields in channel flows generates significant magnetohydrodynamics (MHD) effects, which often result in the need of higher pressure gradients to drive the fluid and lower heat transfer rates due to the laminarization of the flow. Active boundary control, either open-loop or closed-loop, can be employed to overcome this limitation. Open-loop controllers are in general more sensitive to uncertainties of the system, which may result in a poorer performance. Extremum seeking is a powerful tool to tune in real time open-loop controllers, incorporating certain degree of feedback into the control scheme. In this work we combine extremum seeking with a fixed-structure open-loop controller with the ultimate goal of enhancing mixing in a 2D MHD channel by boundary actuation. We show that by carefully tuning the extremum seeking controller the modified open-loop control scheme can be as effective as previously proposed closed-loop control schemes.**

I. Introduction

Magnetohydrodynamic problems arise in many areas. One major application is cooling systems, where electrically conducting fluids are often used as the heat transfer media. Although they are highly favorable for heat transfer due to their excellent thermal properties (high heat conductivity and high boiling point), they also tend to be strongly affected by magnetic fields, which are often present in the system. When an electrically conducting fluid moves in the presence of a transverse magnetic field, it produces an electrical field due to charge separation and subsequently an electric current. The interaction between the induced electric current and the imposed magnetic field originates a body force, called the Lorentz force, which acts on the fluid itself. Because this force acts in the opposite direction of the fluid motion, it is necessary to increase the pressure gradient on the streamwise direction to maintain the mean velocity of the flow and more power is required to pump the liquid through the channel. In addition, this force tends to suppress turbulence and laminarize the flow, reducing the heat transfer rate as a consequence. A good review of the present state of research in this area can be found in [1].

Active control of fluid systems, implemented through micro electro-mechanical (MEM) or electro-magnetic actuators and sensors, can be used to achieve optimally the desired level of stability (when suppression of turbulence is desired) or instability (when enhancement of mixing is desired). The benefits of managing and controlling unsteady flows in engineering applications can be significant. This area has attracted much interest and has dramatically advanced in recent years [2], [3], [4]. The boundary control of MHD flows has been considered for decades [5], [6], [7], [8], [9]. Research subjects range from strongly coupled MHD problems, like liquid metal and melted salt flows, to weakly coupled MHD problems, like salt water flows. Early research mostly focused on passive and open loop control. This situation is partly due to the complexity of the coupled MHD equations.

Our prior work includes the development of a feedback control scheme for mixing enhancement in a 2D MHD flow [10], [11]. Micro-jets, pressure sensors, and magnetic field sensors embedded into the walls of the flow domain were considered in the mentioned work to find a feedback control law that is optimal with respect to a cost functional related to a mixing measure. The effectiveness of the proposed controller has been illustrated in [12], where a simple traveling-wave-like boundary control was also investigated for comparison. The numerical simulations confirmed that the closed-loop control scheme is generally more effective than the simple open-loop controller. However, it was speculated at that time that fine-tuning of the parameters of the open-loop control law could result in an improved performance.

In this work we employ extremum seeking to optimize in real time the performance of an open-loop controller. Extremum seeking is a powerful tool to build a real-time feedback controller based on fixed-structure, open-loop control law with to-be-tuned parameters. The idea of extremum seeking originated decades ago. Recently it has become a popular tool for real-time optimization [13]. It can be used in many nonlinear engineering problems which have local minimums or maximums. Applications of extremum seeking to flow control include [14], [15], [16]. A small sinusoidal perturbation is added to the parameter that is being optimized and the corresponding change of the cost function is processed to decide the optimization direction. The procedure is fully automatic and several parameters can be optimized simultaneously.

However, significant difficulty still remains when using an open-loop scheme to control a complex fluid system. The main problem is due to the multiscale complexity of the MHD channel flow. Our simulation results show that the mixing-related cost function shows highly nonlinear and sometimes nearly discontinuous behavior. This poses serious challenges for extremum seeking, which is essentially a

This work was supported by the NSF CAREER award program (ECCS–0645086). Lixiang Luo (lixiang.luo@lehigh.edu) and Eugenio Schuster (schuster@lehigh.edu) are with the Department of Mechanical Engineering and Mechanics, Lehigh University, Bethlehem, PA 18015, USA.

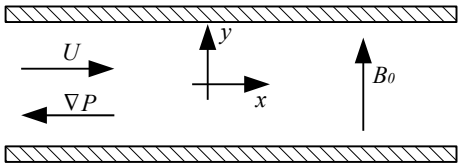

Fig. 1. 2D MHD flow between plates

gradient-based search scheme. Previous work has confirmed that under this circumstances the optimization problem may not be well-posed [17]. On the other hand, our cost function does show a clear trend of being maximized at a certain region. Measures are taken to overcome this difficulty, so that the overall trend of the cost function can be captured regardless of occasional discontinuities.

This article is organized as follows. In Section II, we state the full equation system for incompressible MHD flows, and derive the equations required for numerical simulations. In Section III, the control scheme is presented, including a brief introduction to extremum seeking. In Section IV, simulation results are given for different control schemes in a typical magnetohydrodynamic physical setting. Section V closes the paper stating the conclusion and the identified future work.

II. Problem statement

We consider a 2D, incompressible, electrically conducting fluid flowing between two parallel plates ($0 < x < d = 4\pi$, and $-1 < y < 1$) along the x-direction, as illustrated in Fig. 1, where an external magnetic field B_0 is imposed perpendicularly to the plates, i.e., in the y-direction. This flow was first investigated experimentally and theoretically by Hartmann [18]. The mass flux Q is fixed. A uniform pressure gradient P_x in the x-direction is required to balance the boundary drag force and the body force due to the MHD effects. Space variables x and y, time t, velocity $\mathbf{v}$, magnetic induction $\mathbf{B}$, and current density $\mathbf{j}$ are converted to their dimensionless forms: $x = \frac{x^*}{L}$, $y = \frac{y^*}{L}$, $t = \frac{t^* U_0}{L}$, $\mathbf{B} = \frac{\mathbf{B}^*}{B_0}$, $\mathbf{v} = \frac{\mathbf{v}^*}{U_0}$, $\mathbf{j} = \frac{\mathbf{j}^*}{U_0 B_0}$, where L, U_0 and B_0 are dimensional reference length, velocity and magnetic field. Variables denoted by the star notation are dimensional quantities. The vector variables are defined as $\mathbf{v}(x,y,t) = U(x,y,t)\hat{\mathbf{x}} + V(x,y,t)\hat{\mathbf{y}}$ and $\mathbf{B}(x,y,t) = B^u(x,y,t)\hat{\mathbf{x}} + B^v(x,y,t)\hat{\mathbf{y}}$, where $\hat{\mathbf{x}}$ and $\hat{\mathbf{y}}$ are unit vectors on x and y directions. The dimensionless governing equations for the MHD channel flow are given by

$$\frac{\partial \mathbf{v}}{\partial t} = \frac{1}{\mathrm{Re}}\nabla^2 \mathbf{v} - \nabla P - (\mathbf{v}\cdot\nabla)\mathbf{v} - \mathrm{N}(\mathbf{j}\times\mathbf{B}), \tag{1}$$

$$\frac{\partial \mathbf{B}}{\partial t} = \frac{1}{\mathrm{Re_m}}\nabla^2 \mathbf{B} + \nabla\times(\mathbf{u}\times\mathbf{B}), \tag{2}$$

$$\mathbf{j} = \frac{1}{\mathrm{Re_m}}\nabla\times\mathbf{B}, \tag{3}$$

$$\nabla\cdot\mathbf{v} = 0, \tag{4}$$

$$\nabla\cdot\mathbf{B} = 0. \tag{5}$$

The characteristic numbers, including Reynolds number, magnetic Reynolds number, Alfvén number and Stuart number are defined as: $\mathrm{Re} = \frac{U_0 L}{\nu}$, $\mathrm{Re_m} = \mu\sigma U_0 L$ and $\mathrm{N} = \frac{\sigma B_0^2 L}{\rho U_0}$. The Hartmann number, $\mathrm{Ha} = B_o L\sqrt{\frac{\sigma}{\rho\nu}}$, is used to indicate the interaction level between the magnetic field and the velocity field. The physical properties of the fluid, including the mass density ρ, the dynamic viscosity ν, the eletrical conductivity σ and the magnetic permeability μ, are all assumed constant.

The bottom and top walls are assumed non-slip, perfectly electrically insulating boundaries. Hence, the boundary conditions for the uncontrolled MHD system are given by

$$U(x,\pm1,t) = 0, \qquad V(x,\pm1,t) = V_{ctrl},$$
$$B^u(x,\pm1,t) = 0, \qquad \left.\frac{\partial B^v}{\partial y}\right|_{y=\pm1} = 0,$$

where V_{ctrl} is determined by the proposed boundary control laws. In the uncontrolled cases, $V_{ctrl} = 0$.

In this paper, we consider MHD flows at low magnetic Reynolds numbers, which are also called simplified MHD (SMHD) flows. In these flows the induced magnetic field is neglible in comparison with the imposed magnetic field. The 2D SMHD channel flow is described by slightly modified incompressible N-S equations [19]:

$$\frac{\partial \mathbf{v}}{\partial t} = \frac{1}{\mathrm{Re}}\nabla^2 \mathbf{v} - (\mathbf{v}\cdot\nabla)\mathbf{v} + \nabla P + \mathrm{N}(\bar{U} - U)\hat{\mathbf{x}}, \tag{6}$$

$$\nabla\cdot\mathbf{v} = 0, \tag{7}$$

where $\bar{U}$ represents the average speed, defined as $\bar{U} = Q/L$.

The validity of this simplified MHD model has been verified by many pieces of work [20]. The advantage of using SMHD instead of full MHD is significant, because instead of solving a coupled PDE of the two time-evolving fields ($\mathbf{v}$ and $\mathbf{B}$) with very different time scales, we can solve only one time-evolving field. In most engineering applications, the conditions $\mathrm{Re} \gg 1$ and $\mathrm{Re_m} \ll 1$ hold. Numerical simulations also confirm that under such physical settings, full MHD and SMHD give nearly identical results, while the former method has to use much smaller time steps (characterized by CFL$\ll$1 [21]) than the latter method to ensure convergence [22].

III. Extremum seeking feedback control

The design of the boundary control by extremum seeking starts with a given open-loop control law with undetermined parameters, which are then optimized by the extremum seeking in real time. Although the open-loop control law does not include any information obtained from the system output, the combined control scheme can still drive the system to an optimal state, at least near a local maximum.

The control law, implemented through an array of MEM micro-jets, is given by a traveling wave as the boundary condition:

$$V(x,\pm1,t) = V_{ctrl} = A\sin(kx + \theta t), \tag{8}$$

where constant A is the maximum amplitude, k is the wave number, and θ is the phase speed. The effectiveness of this open-loop control law heavily depends on k and θ. The period of the control "wave" in space is $\lambda = 2\pi/k$, and then the total number of periods is $N_c = \mathrm{L}/\lambda$. In our simulations,

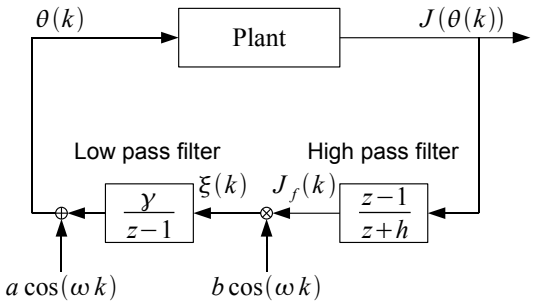

Fig. 2. Extremum seeking control scheme

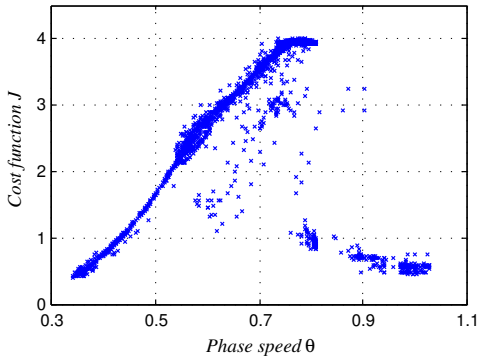

Fig. 3. Enstrophy as a function of phase speed

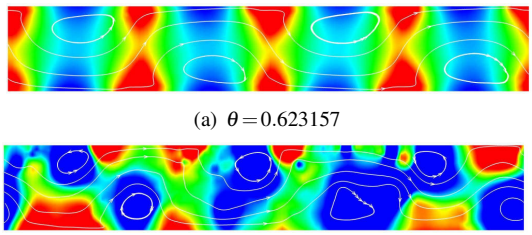

(a) $\theta = 0.623157$

(b) $\theta = 0.623233$

Fig. 4. Streamlines and pressure maps for two cases with very similar θ

$L = 4\pi$, which implies $N_c = 2k$. For the traveling-wave to actuate the traveling vortexes, N_c and θ must be set to some specific combination which can excite a corresponding unstable mode of the MHD flow. In a fully developed flow, the unstable mode with most energy is characterized by large vortexes in a constant number traveling in a roughly constant speed downstream. Assume that the average phase speed of the vortexes is V_e and the number of vortexes on one side is N_e, which is half of the total number of vortexes since they appear in pairs on two sides. Ideally, an open-loop controller exciting the unstable mode with most energy will fulfill the condition: $N_c = N_e$ and $\theta = V_e$. In fact, the choices of wave number k are limited to a small number of integers corresponding to the dominant Fourier modes. In this work, we use $k = 1$ because it produces the same number of major vortices as most fully developed flows do (see Fig. 6 for a typical flow pattern). However, without appropriate sensors and real-time spectrum analysis, the actual value of V_e can not be determined precisely, rendering the open-loop controller always out of synchronization with the traveling vortexes.

It is natural for us to seek a scheme that can automatically adjust these parameters in order to drive the system to an optimal or suboptimal state. Optimization methods based on physical models are mostly useless in our problem, because it is very difficult to build a model that is able to represent the relation between the simple control action and the complex fluid system. Hence, model-less schemes have to be considered. Extremum seeking is a model-less real-time optimization scheme which is effective for a wide range of linear and nonlinear optimization problems, making itself an ideal candidate for our problem.

Fig. 2 illustrate the extremum seeking scheme as a block diagram. In our problem, extremum seeking is used for iterative optimization of the phase speed θ in order to match the phase speed of the boundary control with the phase speed of the major vortices in the flow, so that the mixing effect can be maximized. We use the enstrophy, a good indicator of turbulence inside the flow,

$$E_s(v) = \frac{1}{2d}\int_{-1}^{1}\int_{0}^{d}\frac{1}{2}\left(\frac{\partial v}{\partial x} - \frac{\partial u}{\partial y}\right)^2 dxdy, \qquad (9)$$

to measure the level of mixing effect. At the beginning of each extremum seeking iteration, a phase speed $\theta(k)$, superposed by an intentional sinusoidal perturbation (modulation), is fed into the flow system. The simulation of flow system runs with the new phase speed until its cost function reaches a statistically steady state. We take samples of the enstrophy every 20 simulation steps and calculate the standard deviation of the last 200 samples. A flow is considered statistically steady if this standard deviation decreases to a specific level. The system output $J(\theta(k))$ is then given by the enstrophy, averaged over the same period of time during which the standard deviation is computed. The system output is filtered by a high-pass filter and multiplied by another sinusoidal signal (demodulation). The resulting signal is filtered through a low-pass filter, which becomes the new phase speed for the next iteration. More details on the theory behind this scheme can be found in [13].

For a continuous function of a single variable, with well-defined maximum points, extremum seeking is very effective. Given the right parameters and enough iterations, the scheme can almost guarantee convergence, at least to a local maximum. However, if the cost function is not very smooth or even discontinuous, then the extremum seeking algorithm may not capture the slope information and fails. Such problems do arise in our work, as the cost function has many sudden changes near the optimal point. The complexity of the cost function can be seen in Fig. 3. The simulations are done with the following parameters: $\mathrm{Re} = 6000$, $\mathrm{B}_0 = 0.3$ and $\mathrm{N} = 0.002$. While the cost function shows a clear trend of being maximized around 0.75, it seems extremely sensitive to the phase speed. This behavior is largely caused by the nonlinearity of the flow. To achieve higher enstrophy, the boundary control has to produce large sustained vortices in the flow. Due to its nonlinearity nature, the development of vortices is seriously affected by the initial conditions and random numerical noise. It may take extensive long time for the flow to reach the statistically steady state. Furthermore,

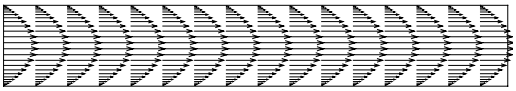

Fig. 5. Initial velocity field (Re = 7500)

a flow with specific physical settings may have more than one statistically steady state and may not converge to the one with the highest enstrophy. Take two data points in Fig. 3 for example, the steady state enstrophy drops by 72% from 2.92×10^7 to 8.13×10^6 while the phase speed increases by 0.012% from 0.623157 to 0.623233. The pressure maps and stream lines in Fig. 4 indicate that the vortex patterns in the two cases are completely different. While the case with much higher enstrophy have four sustained organized vortices, the case with much smaller enstrophy has three smaller deformed vortices on each side. Since the boundary control has two periods on the streamwise direction, the pattern of three vortices does not match the period of the boundary control, which means the boundary control is out of synchronization and contributes very little to the increase of turbulence.

The mechanism of this irregular behavior of the cost function is not clearly understood and it will not be discussed in detail in this work. However, a special technique has to be implemented within the extremum seeking algorithm to eliminate the undesirable effect of the discontinuity. This technique is based on the assumption that in the sense of overall trend the cost function does not change significantly. First, we reduce the perturbation signal $a\cos(\omega k)$ in the region with significant discontinuity, such that the cost function be expected to change slightly at every extremum seeking iteration. A simple low-pass filter is then added immediately after the plant output. This filter provides the average of the most recent 5 plant outputs $J(\theta(k))$ (including the latest plant output). This average can eliminate most of the discontinuity while capturing the overall trend, thus increasing the ability of the extremum seeking to stay inside the optimal region.

IV. Simulation Results

The numerical simulations are carried out by a modified Navier-Stokes solver. The equations are discretized using FFT on the streamwise direction and finite differences on the spanwise direction, which is also called the pseudospectral method. Time integration is done using a fractional step method along with a hybrid Runge-Kutta/Crank-Nicolson scheme. Linear terms are treated implicitly by the Crank-Nicolson method and nonlinear terms are treated explicitly by the Runge-Kutta method. The divergence-free condition is fulfilled by the fractional step method.

All the simulations are carried out for the same flow domain: $-1<y<1$, $0<x<4\pi$. The same mesh is used in all the simulations presented in this section (grid points in the x direction: NX = 150, grid points in the y direction: NY = 128).

A. MHD flows with no control

When $B_0=0$ (Ha$=0$), the momentum equation (1) reduces to the well-known Navier-Stokes equation. The two-dimensional channel flow, which is also known as the Poiseuille flow, is frequently cited as a paradigm for transition to turbulence, and has drawn extensive attention through the history of fluid dynamics. This is a classical flow control problem that has been studied in [4] and the references therein assuming the availability of an array of pressure sensors on the walls and an array of MEM micro-jet actuators (also distributed along the walls) capable of blowing/suction. Incompressible conventional flows in 2D channels can be linearly stable for low Reynolds numbers, as infinitesimal perturbations in the flow field are damped out. The flows turn linearly unstable for high Reynolds numbers (Re>5772) [23], [24]. Such flows usually reach statistically steady states, which we call fully established flows. Fig. 5 and Fig. 6 show how a channel flow (Re$=7500$) develops to a fully established flow. The initial parabolic equilibrium velocity profile, which is linearly unstable, is shown in Fig. 5. The pressure maps and streamlines, given by Fig. 6, illustrate how the vortices evolve in time until reaching a fully established flow when the initial equilibrium velocity profile is infinitesimally perturbed at $t=0$.

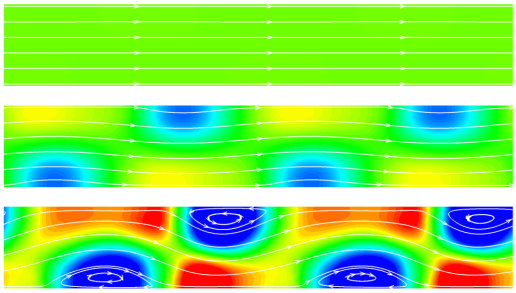

Fig. 6. Pressure maps and streamlines for Re = 7500 (t =266, 1590, 2973)

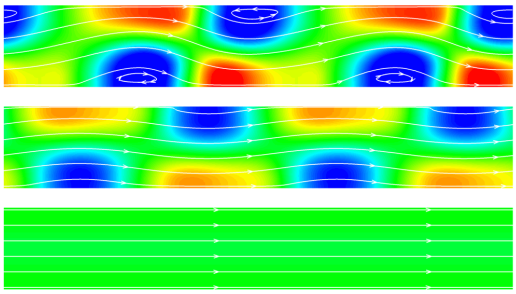

Fig. 7. Pressure maps and streamlines for Re$=7500$, Ha$=1.83$ (t=144, 945, 1126 after the magnetic field is imposed)

When $B_0\neq0$ (Ha$\neq0$), Fig. 7 shows the effect of the imposed transverse magnetic field on the stability properties of the flow. Vorticity maps obtained through direct numerical simulation studies show the stabilizing effect of the imposed magnetic field on the 2D Hartmann flow. The simulation is started at $t=0$ with the fully established flow achieved in Fig. 6. The enstrophy is commonly used to quantify the overall turbulence of the velocity field. In our work we use the averaged enstrophy, defined by (9). The enstrophy of the simulation case shown in Fig. 7, whose curve can be found in Fig. 8 labeled "Ha$=1.83$ ", decreases as the flow is stabilized by the imposed magnetic field. Also, stronger imposed magnetic fields tend to make the flow more stable, as shown in the same figure.

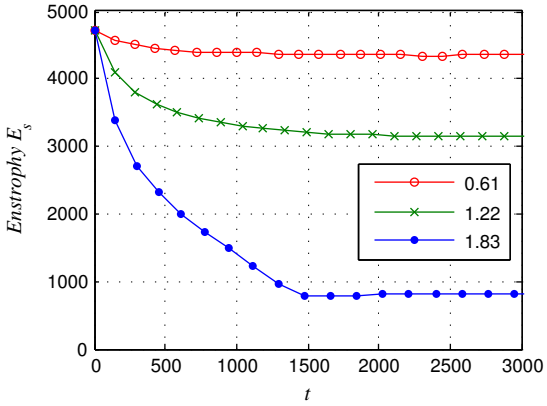

Fig. 8. Enstrophy as function of time for different imposed magnetic fields

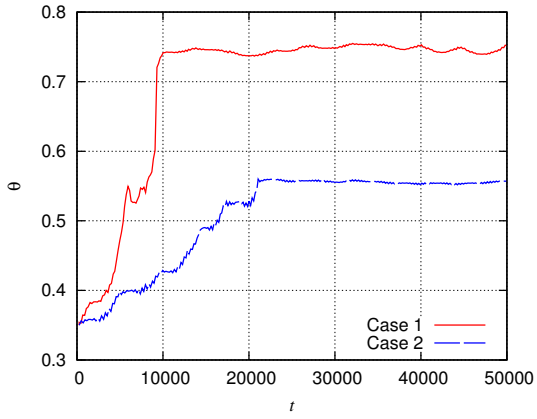

Fig. 9. Phase speed development for extremum seeking feedback control

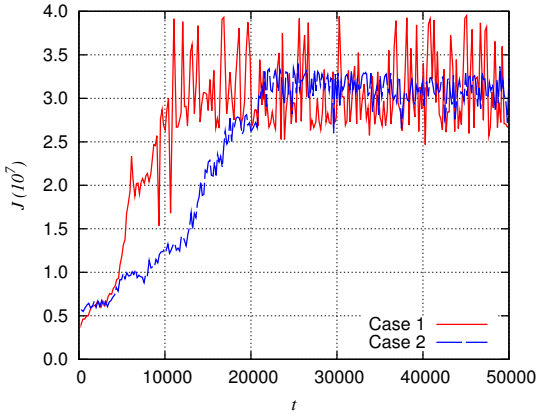

Fig. 10. Enstrophy development for extremum seeking feedback control

B. MHD flows with extremum seeking feedback control

In this section, the boundary control based on extremum seeking is tested. The simulations all start with equilibrium solutions achieved after an external magnetic field is imposed. These flows remain linearly stable indefinitely if no boundary control is present. The boundary control is expected to drive these flows to states with higher enstrophy levels, thus enhancing mixing. Simulations are conducted for these parameters:

- Case 1: Re$=6000$, $Q=1.5$, Ha$=1.04$.
- Case 2: Re$=7500$, $Q=1.5$, Ha$=1.83$

The initial phase speed is set to 0.35 for both simulation cases. The other parameters are set as $A=0.05$, $k=4$. The parameters for extremum seeking have to be carefully chosen to balance the stability and performance of the optimization process. In this case, we use $a=0.004$ for $\theta<0.5$ and $a=0.002$ for $0.5<\theta<0.9$. Other parameters are set as $b=1$, $\omega=3$, $\gamma=10^{-9}$ and $h=0.8$.

As we can see in Fig. 9 and Fig. 10, the boundary control based on extremum seeking gradually modifies the phase speed to try to maximize the cost function. Even though the control can not stay at the optimal phase speed all the time, it manages to stabilize the phase speed near the maximum region, regardless significant amount of randomness in the cost function.

Results of simulations with the same physical parameters, but using a feedback control law, are also given for comparison. The feedback boundary control actuation proposed in [10], [11] is determined by both the pressure field and the magnetic field:

$$V_{ctrl} = -k_p \Delta p - k_b \Delta B^{v2}, \tag{10}$$

where k_p and k_b are constants used to represent the control gains, and

$$\Delta p = p(x,1,t) - p(x,-1,t),$$
$$\Delta B^{v2} = (B^v(x,1,t))^2 - (B^v(x,-1,t))^2.$$

Note that the simulations under this control requires a full MHD solver, which was developed as part of our previous work [12]. Since the feedback control law (10) does not involve any real-time optimization process, it provides the full control effort much more quickly than the extremum-seeking-based controller. However, as we will see from the simulation results, the extremum-seeking-based controller can maintain a higher enstrophy level. The gains of the feedback control are set as $k_p=0.1$, $k_b=10000$. Since the two control laws are very different in nature, it is hard to compare them side-by-side. Instead, we compare the enstrophy level for similar control efforts, defined as

$$C(\mathbf{v}) = \frac{1}{d}\int_0^d V(x,-1,t)^2 + V(x,1,t)^2 dx. \tag{11}$$

As illustrated in Fig.11 and Fig.12, the average control effort and resulting enstrophy of the flow with Re$=6000$, controlled by the boundary control law (10), is 0.11 and 2.5×10^6, which gives a enstrophy-control ratio J/C of around 2.2×10^7. The extremum-seeking-based controller has a constant control effort, regardless of the phase speed. In the case shown in Fig. 9 and Fig. 10, the control effort is 0.217, while the average enstrophy is 2.6×10^7. This gives a much higher J/C ratio of around 1.2×10^8, 5 times higher than the one given by control law (10). A further investigation reveals that the flow controlled by (10) does not have sustained large vortices like Fig. 4(a). Instead, its flow pattern is more similar to Fig. 4(b), resulting in a relatively low enstrophy level.

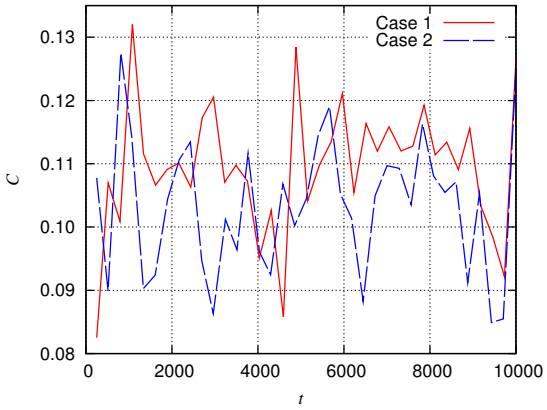

Fig. 11. Control effort for boundary feedback control

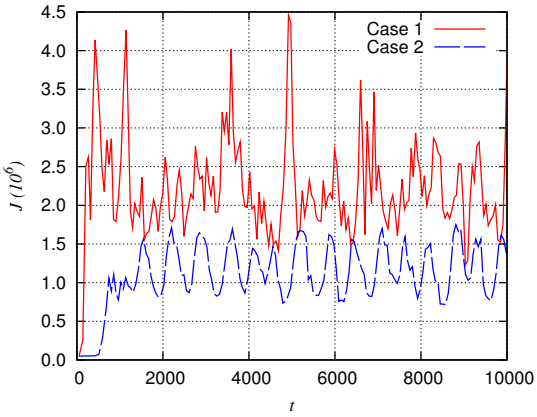

Fig. 12. Enstrophy development for boundary feedback control

Similar results can be found in the case with Re = 7500. As shown in Fig.9 and 10, the phase speed under the regulation of extremum seeking is successfully optimized around 0.55. A flow with the same physical parameters and a control by control law (10) uses similar control effort (around 0.1) but much lower enstrophy level (around 2.5×10^6), as shown in Fig. 11 and Fig. 12. Hence, with Re = 7500, the enstrophy-control ratio J/C given by two control schemes is also differed significantly: 1.4×10^8 in case with extremum seeking scheme and 2.5×10^7 in the case with feedback control law (10).

V. Conclusion

In this work, we developed a boundary controller for mixing enhancement in a 2D MHD channel flow. The controller is based on a modified open-loop boundary controller whose parameters are regulated by extremum seeking. The simulation results show that the controller successfully increases the enstrophy level of the otherwise linearly stable flow, thus increasing mixing effects inside the flow. The tuning of the extremum seeking scheme is crucial for the success of the controller. Because of the complexity of the MHD channel flow, significant discontinuities exist in the relationship between the to-be-maximized cost function and the to-be-optimized parameters. A simple but effective method based on averaging is used to avoid disruptions caused by cost function discontinuities during the extremum-seeking optimization process. Results show that the extremum-seeking-based controller could be as effective in maintaining high mixing levels as a previously proposed feedback control scheme.

In our future research, the extremum-seeking-based control scheme will be extended to 3D MHD flows. It may be also necessary to develop alternative methods to deal with the discontinuity of the cost function, especially when the number of parameters being optimized is more than one.

References

[1] U. Müller and L. Bühler, *Magnetofluiddynamics in channels and containers*. Springer, 2001.

[2] M. D. Gunzburger, *Flow Control*, ser. The IMA Volumes in Mathematics and its Applications. New York: Springer-Verlag, 1995, vol. 68.

[3] S. S. Sritharan, Ed., *Optimal control of viscous flow*. SIAM, Philadelphia, 1998.

[4] O. M. Aamo and Krstić, *Flow Control by Feedback*. Springer, 2002.

[5] A. B. Tsinober, *Viscous Drag Reduction in Boundary Layers*, ser. Progress in Astronautics and Aeronautics. Washington, DC: AIAA, 1990, no. 123, ch. MHD flow drag reduction, pp. 327–349.

[6] C. Henoch and J. Stace, "Experimental investigation of a salt water turbulent boundary layer modified by an applied streamwise magnetohydrodynamic body force," *Physics of Fluids*, vol. 7, no. 6, pp. 1371–1383, June 1995 1995.

[7] H. Choi, D. Lee, and J. Lim, "Control of near-wall streamwise vortices using an electromagnetic force in a conducting fluid," *AIAA Paper*, vol. 97, p. 2059, 1997.

[8] T. Berger, J. Kim, C. Lee, and J. Lim, "Turbulent boundary layer control utilizing the Lorentz force," *Physics of Fluids*, vol. 12, p. 631, 2000.

[9] E. Spong, J. Reizes, and E. Leonardi, "Efficiency improvements of electromagnetic flow control," *Heat and Fluid Flow*, vol. 26, pp. 635–655, 2005.

[10] E. Schuster and M. Krstić, "Inverse optimal boundary control of mixing in magnetohydrodynamic channel flows," *Proceedings of the 42nd IEEE Conference on Decision and Control*, 2003.

[11] E. Schuster, L. Luo, and M. Krstic, "Mhd channel flow control in 2d: Mixing enhancement by boundary feedback," *Automatica*, vol. 44, no. 10, pp. 2498 – 2507, 2008.

[12] L. Luo and E. Schuster, "Heat transfer enhancement in 2D magnetohydrodynamic channel flow by boundary feedback control," *45th IEEE Conference on Decision and Control*, p. 5317, San Diego, 2006.

[13] K. Ariyur and M. Krstić, *Real-time optimization by extremum-seeking Control*. Wiley-Interscience, 2003.

[14] R. King, R. Becker, G. Feuerbach, L. Henning, R. Petz, W. Nitsche, O. Lemke, and W. Neise, "Adaptive flow control using slope seeking," *14th Mediterranean Conference on Control and Automation*, pp. 1–6, June 2006.

[15] R. Becker, R. King, R. Petz, and W. Nitsche, "Closed-loop separation control on a high-lift configuration using extremum seeking," *AIAA Journal*, vol. 45, no. 6, pp. 1382–1392, June 2007.

[16] J. F. Beaudoina, O. Cadotb, J. L. Aiderc, and J. E. Wesfreid, "Bluff-body drag reduction by extremum-seeking control," *Journal of Fluids and Structures*, vol. 22, no. 6-7, pp. 973 – 978, 2006.

[17] B. Protas, T. Bewley, and G. Hagen, "Some formulation issues in adjoint-based optimal estimation and control of PDEs," (preprint).

[18] J. Hartmann, *Theory of the laminar flow of an electrically conductive liquid in a homogeneous magnetic field*, xv(6) ed. Det Kgl. Danske Vidensk-abernes Selskab. Mathematisk-fysiske Meddelelser.

[19] G. Branover, *Magnetohydrodynamic flow in ducts*. Halsted Press, 1979.

[20] D. Lee and H. Choi, "Magnetohydrodynamic turbulent flow in a channel at low magnetic reynolds number," *Journal of Fluid Mechanics*, vol. 439, pp. 367–394, 2001.

[21] J. Anderson, *Computational fluid dynamics, the basics with applications*. McGraw-Hill, 1995, pp. 153–165.

[22] H. Choi and P. Moin, "Effects of the computational time step on numerical solutions of turbulent flow," *Journal of Computational Physics*, vol. 113, no. 1, pp. 1–4, 1994.

[23] R. L. Panton, *Incompressible flow*, 2nd ed. New York: Wiley, 1996.

[24] P. J. Schmid and D. S. Henningson, *Stability and transition in shear flows*. New York: Springer, 2001, vol. 142.